Interaction of Metal Phthalocyanines with Carbon *Zigzag* and *Armchair* Nanotubes with Different Diameters

Pavel O. Krasnov[1,2,*], Tamara V. Basova[3,4], Aseel Hassan[5]

[1]Institute of Nanotechnology, Spectroscopy and Quantum Chemistry, Siberian Federal University, Krasnoyarsk, 660041, Russia

[2]Reshetnev Siberian State University of Science and Technology, Krasnoyarsk, 660049, Russia

[3]Nikolaev Institute of Inorganic Chemistry SB RAS, Novosibirsk, 630090, Russia

[4]Novosibisrk State University, Novosibirsk, 630090, Russia

[5]Material and Engineering Research Institute, Sheffield Hallam University, Sheffield, UK

Abstract

Quantum-chemical calculations of the association of metal free, cobalt, copper and zinc phthalocyanines (MPc) with carbon *zigzag* and *armchair* nanotubes (CNTs) with diameters in the range of 7-14 Å were carried out by the DFT method with the use of BH van der Waals density functional and DZP atomic basis set. It was shown that interaction energy between the phthalocyanine molecules and the CNTs, as a whole, increases with an increase of the diameter of carbon nanotubes. However, in the case of CNT(n,0) the energy reaches its maximal value at n = 16 or 17 depending on the central metal atom and phthalocyanine orientation on the carbon nanotubes surface. Up to diameter of 10.5 Å of the CNTs, stronger binding of the considered MPc macrocyclic molecules is observed with carbon *armchair* nanotubes. However, in the case of higher diameters the phthalocyanines are associated more strongly with the *zigzag* CNTs.

Keywords: phthalocyanines; carbon nanotubes; π-π-stacking; density functional theory; dispersion correction; basis set superposition error.

1. Introduction

Hybrid materials nowadays are well known materials studied and used for the development of photovoltaic devices as well as several other technological applications. As an example of such materials are those consisting of an inorganic part represented by carbon nanostructures such as fullerenes or carbon nanotubes (CNTs), and an organic part, e.g. phthalocyanine or porphyrin or their metal complexes. Over the last 10 years several tens of reviews [1-12] have been written summarizing numerous original works carried out and are devoted to the study of these hybrid materials and their

[*] Corresponding author – e-mail: kpo1980@gmail.com, phone: +79080209830

practical applications. In these materials the macrocyclic molecules play the role of electron donors whereas carbon nanostructures are electron acceptors. The light adsorption leads to electrons transfer from the organic component to the inorganic part, with the formation of systems with separated charges. This phenomenon is useful for the operation of the solar cells. Apart from photovoltaic applications, these materials can also be used in different technological areas such as chemical and biological sensors, nanoelectronic devices, fuel cells, and so on [13,14].

Porphyrins or phthalocyanines can bind with fullerenes and carbon nanotubes via either covalent or non-covalent interactions [15], where in the last case, π-π-stacking arises between the aromatic rings. This type of interaction is one of the examples of supramolecular interaction which plays an important role in materials science because it plays a role of driving force in such processes as molecular self-assembly.

It is necessary to mention that in the case of formation of hybrids of carbon nanotubes with the above mentioned macrocyclic molecules, the CNT size and its type of chirality as well as the nature of the central metal atoms and substituents in the phthalocyanine and porphyrin molecules have a significant effect on the strength of bonding between these two components [16,17].

DFT quantum-chemical calculations, performed by Zhao and Ding [18], have demonstrated that the strongest binding energy was observed in the case of semiconducting carbon nanotubes than in the case of metallic ones. The authors have compared the interaction of CNT(6,6) and CNT(10,0) with the cobalt, zinc, nickel and copper porphyrins (CoP, ZnP, NiP and CuP, respectively). At the same time, Alvarez *et al.* have concluded that the electronic properties of carbon nanotubes do not play a significant role in the interaction with phthalocyanines molecules [19]. According to their study, the diameter of CNTs has more significant effect, leading to an increase of the distortion of the macrocyclic plane with decreasing carbon nanotubes diameter. A strong distortion of metal free phthalocyanine (H_2Pc) interacting with CNT(5,5) and CNT(10,0) was observed by Chávez-Colorado and Basiuk [20]. According to their study this phenomenon allows H_2Pc to increase its contact area with the carbon nanotube sidewalls. Correa and Orellana have also observed a distortion of the macrocyclic molecules upon adsorption of metal free porphyrin and phthalocyanine as well as their Zn complexes onto the surface of CNT(14,0) [21]. The strong interaction of copper and zinc phthalocyanines with CNT(5,5) and CNT(10,0) was also demonstrated by Basiuk *et al.* [22], where the binding energies are in diapason from 1.41 eV (32.46 kcal/mol) to 1.61 eV (37.12 kcal/mol).

In addition, porphyrins and phthalocyanines as well as their metal complexes can have different orientations on the carbon nanotube surface [21,23]. The energy difference between the two types of macromolecules depends both on the nature of the central metal atom and the nature of macrocyclic molecule. If a porphyrin or a phthalocyanine molecule possesses an electric charge, being a cation, it binds to the carbon nanotube stronger than those in the neutral form [24]. Zhao and Ding have demonstrated that the binding energy of CoP with CNT(6,6) and CNT(10,0) is higher compared to

ZnP, NiP and CuP. In the case of CNT(10,0) the interaction strengths with the zinc, nickel and copper porphyrins are almost equal [18]. At the same time, the binding energy of CNT(6,6) with NiP is a little bit higher than that with ZnP and CuP. Correa and Orellana have shown that the binding energy of phthalocyanines with CNT(14,0) is higher than in the case of the corresponding porphyrins, and the interaction between carbon nanotubes and their zinc complexes is stronger than with metal-free molecules [21].

Despite of the above-described work, it still remains unclear how the interaction between the phthalocyanines and carbon nanotubes depends on the size and chirality of the latter, and which orientation of the macrocylic molecules on CNT surface is more favorable.

In this work, we use DFT quantum-chemical calculations to study the interaction between metal phthalocyanines (MPc, where M = H_2, Co, Cu and Zn) and carbon *zigzag* and *armchair* nanotubes with diameters in the range 7-14 Å.

2. Computational details

Metal free phthalocyanine (H_2Pc) and its complexes with cobalt, copper and zinc (MPc, where Me = Co, Cu and Zn) were chosen to study the effect of the central atom on the interaction with *zigzag* and *armchair* nanotubes with diameter (*d*) in the range 7-14 Å, i.e. CNT(n,0), where $n = 9 \div 18$, and CNT(m,m), where $m = 5 \div 10$, respectively.

In a similar manner to the case of metal free phthalocyanine described by Correa and Orellana [21], three possible orientations of H_2Pc molecule on the carbon nanotubes surface are considered: N-H bonds form an angle of 45º with the CNT axis (Position 1), N-H bonds are parallel to the CNT axis (Position 2) and N-H bonds are perpendicular to this CNT axis (Position 3), as illustrated in Fig. 1. The second and third orientations are equivalent in the case of metal phthalocyanine, therefore only Position 1 and Position 2 are considered for MPc (M = Co, Cu and Zn).

The two inner hydrogen atoms of free-base phthalocyanine in real-life can migrate from one pair of nitrogen atoms to the other [25]. From this point of view, Position 2 and Position 3 of H_2Pc are not exact structures existing separately, they can be considered as two tautomeric forms of free-base phthalocyanine with the different positions of inner hydrogen atoms.

Quantum-chemical simulation is carried out by the DFT method for the considered compounds geometry and nature of phthalocyanines interaction with the carbon nanotubes with the use of BH van der Waals density functional [26-28] and DZP atomic basis set [29-30] (DFT BH/DZP method). All calculations were performed with a SIESTA software package [31] as spin unpolarized, using the pseudo potentials. In this approach the internal electrons of atoms are not considered separately, but they together with the atomic nucleus represent an ion with which external electrons interact.

During optimization of the geometrical structure of all compounds the *k*-point samplings of the first Brillouin zone (1BZ) were chosen as a $1 \times 1 \times 5$ mesh (the CNT axis is directed along *z*-axis)

according to the Monkhorst-Pack scheme [32]. The geometry relaxation was carried out by conjugate gradient minimization until the forces acting on the atoms became less than 0.05 eV/Å.

All investigated structures were considered within the supercell approach (Fig. 1) with periodic boundary conditions along the axes of the carbon nanotubes. The length of translation vector in the case of CNT(n,0) and their aggregates with phthalocyanines was equal to 6a (a is a unit cell length of a carbon nanotube along its axis), while in the case of CNT(m,m) it was equal to 11a, where a values were preliminary calculated for separate CNTs (Table 1). In order to avoid any interaction between the structure images along the x and y axes, the vacuum gap between them was specified. In the case of separate carbon nanotubes vacuum gap is equal to 5a or 6a for *zigzag* CNT depending on their diameter and 9a or 11a for *armchair* CNT, while in the case of MPc/CNT aggregates these values are equal to 6a or 7a and 11a or 13a, respectively. The diameter d of CNTs was defined as the double average distance from the nanotube axis to every atom.

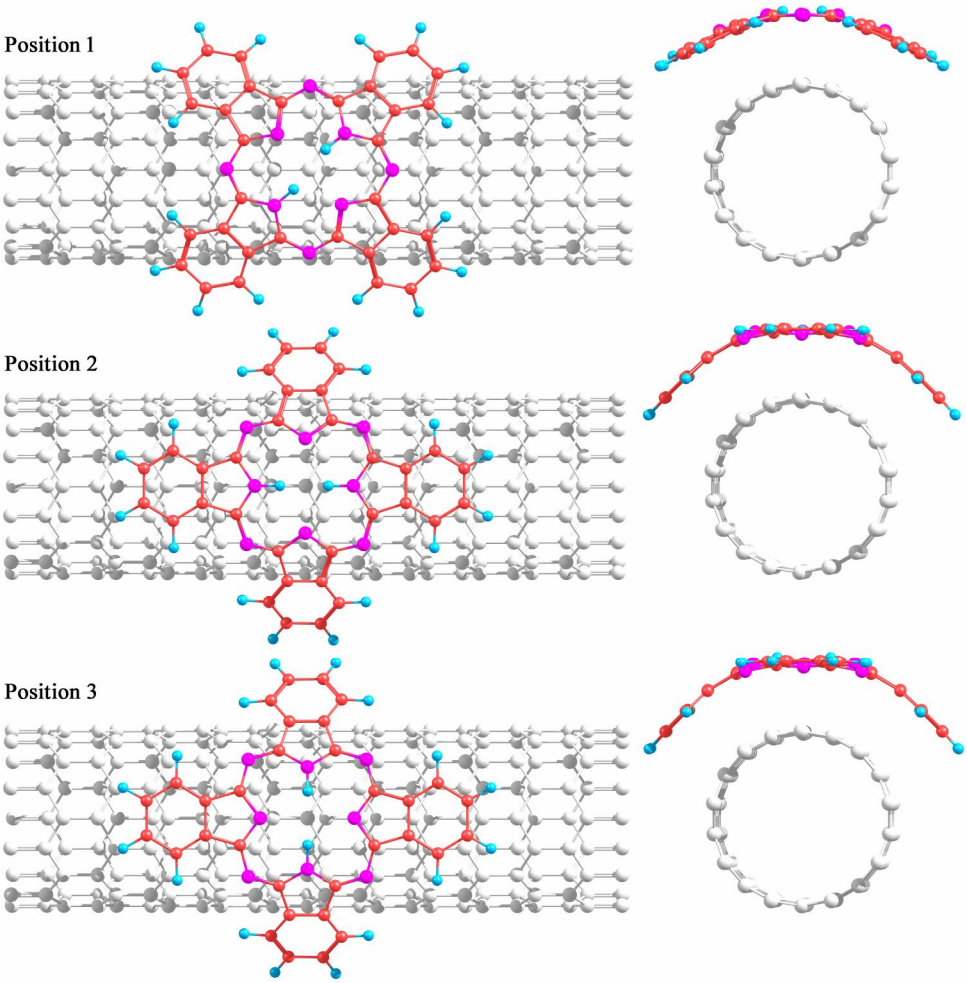

Figure 1 – Three possible positions of H_2Pc on the CNT(9,0) surface

Additionally for comparison purposes analogous calculations were performed for two possible orientations of MPcs on a graphene layer (Fig. S1, Supplementary Material) as an example of a carbon nanotube with infinite diameter. In this case the k-point samplings of the first Brillouin zone (1BZ)

were chosen as a 5 × 5 × 1 mesh (*z*-axis is perpendicular to the carbon surface). The length of translation vector was equal to 11*a*, where value *a* = 2.476 Å was also preliminary calculated for the graphene unit cell. The vacuum gap between the structure images along *z*-direction was equal to 9*a* to avoid their interaction.

Table 1 – Unit cell lengths of carbon nanotubes along their axes

CNT	(9,0)	(10,0)	(11,0)	(12,0)	(13,0)	(14,0)	(15,0)	(16,0)
a, Å	4.283	4.283	4.283	4.296	4.283	4.294	4.294	4.294
d, Å	7.16	7.95	8.73	9.48	10.29	11.05	11.83	12.61
CNT	(17,0)	(18,0)	(5,5)	(6,6)	(7,7)	(8,8)	(9,9)	(10,10)
a, Å	4.283	4.283	2.464	2.472	2.472	2.471	2.470	2.468
d, Å	13.43	14.22	6.93	8.27	9.63	10.99	12.35	13.72

The binding energy between the phthalocyanine molecules and the carbon nanotubes was estimated as a difference of the total energies of the MPc/CNT aggregate components and the MPc/CNT itself:

$$E_b = E_{\mathrm{MPc}} + E_{\mathrm{CNT}} - E_{\mathrm{MPc/CNT}} - \Delta E_{\mathrm{BSSE}}, \quad (1)$$

where ΔE_{BSSE} is the correction to the binding energy, taking into account the basis set superposition error, that was calculated using Equation 2:

$$\Delta E_{\mathrm{BSSE}} = \left(E_{\mathrm{CNT}}^{\mathrm{MPc/CNT}} + E_{\mathrm{MPc}}^{\mathrm{MPc/CNT}}\right) - \left(E_{\mathrm{CNT}^*}^{\mathrm{MPc/CNT}} + E_{\mathrm{MPc}^*}^{\mathrm{MPc/CNT}}\right). \quad (2)$$

Herein the upper index (MPc/CNT) shows that the geometries of CNT and MPc were taken from the optimized geometry of the aggregates of CNT with MPc, however optimization of the geometries of separate components was not performed, but only calculations of energies were carried out. The asterisks in the lower indices mean which component of the MPc/CNT aggregate is considered, whereas the atoms of the other component are dummy atoms are considered as the points described by the corresponding atomic basis sets.

3. Results and discussion

As a result of the performed calculations, it was shown that in general, the strength of MPc binding with CNTs increases with the increase in the diameter of the carbon *zigzag* nanotubes (Table 2). However this effect is observed to have occurred only until CNT reaches a particular size. For example, the largest binding energy of H_2Pc and CoPc is characteristic for CNT(16,0) and CNT(17,0) depending on the phthalocyanine orientation, whereas in the case of both CuPc and ZnPc orientations the largest E_b value is observed for the aggregate with CNT(16,0). At the same time the binding energies of MPcs with graphene are higher and vary in the range from 2.2 eV (50.7 kcal/mol) to 2.6 eV (60.0 kcal/mol) depending on the nature of the central metal and phthalocyanine orientation

(Table S1, Supplementary Material). Therefore it is expected that for carbon nanotubes with diameters larger than 14 Å the strength of phthalocyanine binding will also continue to increase with the increase in the CNT diameter, reaching the values typical for graphene.

In most cases, Position 1 (Fig. 1) is the most energetically preferable orientation of H_2Pc, CuPc and ZnPc on carbon nanotubes surface, except for the association of CuPc with CNT(11,0). The most preferable orientation of H_2Pc in the aggregates with CNT(11,0) and CNT(17,0) is Position 2, and with CNT(14,0) and CNT(18,0) is Position 3 (Fig. 1). CoPc adsorbs on the surface of CNT from (9,0) to (12,0) preferably in Position 1, while it orients on the surface of other *zigzag* carbon nanotubes in the Position 2. In the case of ZnPc, adsorbtion onto the surface of CNT(14,0) Position 1 is energetically more stable, which is in good agreement with the results published elsewhere [21]. On the contrary to the results obtained by Correa and Orellana [21], the preferable orientation of H_2Pc is Position 3 (vs. Position 1 [21]).

Table 2 – Binding energies of phthalocyanines with *zigzag* carbon nanotubes in eV (in kcal/mol)

CNT	CoPc		CuPc		ZnPc		H_2Pc		
	Position 1	Position 2	Position 1	Position 2	Position 1	Position 2	Position 1	Position 2	Position 3
(9,0)	0.95 (21.9)	0.84 (19.4)	0.72 (16.6)	0.47 (10.8)	0.74 (17.1)	0.52 (12.0)	0.63 (14.5)	0.50 (11.5)	0.44 (10.1)
(10,0)	0.74 (17.1)	0.71 (16.4)	0.69 (15.9)	0.58 (13.4)	0.76 (17.5)	0.55 (12.7)	0.66 (15.2)	0.56 (12.9)	0.52 (12.0)
(11,0)	0.96 (22.1)	0.91 (21.0)	0.81 (18.7)	0.93 (21.4)	0.86 (19.8)	0.81 (18.7)	0.81 (18.7)	0.85 (19.6)	0.85 (19.6)
(12,0)	1.03 (23.8)	0.90 (20.8)	0.87 (20.1)	0.60 (13.8)	0.92 (21.2)	0.57 (13.1)	0.77 (17.8)	0.54 (12.5)	0.54 (12.5)
(13,0)	0.83 (19.1)	0.92 (21.2)	0.81 (18.7)	0.77 (17.8)	0.88 (20.3)	0.74 (17.1)	0.72 (16.6)	0.71 (16.4)	0.69 (15.9)
(14,0)	1.30 (30.0)	1.33 (30.7)	1.17 (27.0)	1.09 (25.1)	1.18 (27.2)	1.11 (25.6)	1.03 (23.8)	1.05 (24.2)	1.10 (25.4)
(15,0)	1.40 (32.3)	1.45 (33.4)	1.30 (30.0)	1.09 (25.1)	1.31 (30.2)	1.12 (25.8)	1.16 (26.8)	1.09 (25.1)	1.09 (25.1)
(16,0)	1.60 (36.9)	1.38 (31.8)	1.58 (36.4)	1.18 (27.2)	1.59 (36.7)	1.21 (27.9)	1.45 (33.4)	1.14 (26.3)	1.19 (27.4)
(17,0)	1.33 (30.7)	1.70 (39.2)	1.25 (28.8)	1.14 (26.3)	1.25 (28.8)	1.19 (27.4)	1.12 (25.8)	1.41 (32.5)	1.16 (26.8)
(18,0)	1.30 (30.0)	1.37 (31.6)	1.13 (26.1)	1.11 (25.6)	1.15 (26.5)	1.15 (26.5)	1.00 (23.1)	1.06 (24.4)	1.10 (25.4)

A comparison of the relation between the binding energy values and the most favorable orientation of MPcs on CNT diameters (Fig. 2), it can generally be concluded that E_b decreases in the order CoPc > ZnPc > CuPc > H_2Pc, however, in a number of cases this regularity is violated. For example, the binding strength of ZnPc by CNT(10,0) is a little bit higher, than in the case of CoPc, whereas CuPc is associated with CNT(11,0) more strongly than ZnPc. In the case of CNT(17,0) the binding energy of H_2Pc exceeds the E_b values for CuPc and ZnPc. In general, it can be noted that in the range from CNT(14,0) to CNT(18,0) the bonding strengths of CuPc and ZnPc are very close.

The values of ZnPc and H_2Pc binding energy with CNT(14,0) estimated in this work are lower than those presented by Correa and Orellana [21]. The values of ZnPc binding energy were previously estimated to be 1.55 eV (35.7 kcal/mol) and 1.58 eV (36.4 kcal/mol) depending on its orientation on

CNT surface [21]. At the same time, it was shown that the binding energy of H_2Pc varies from 1.50 eV (34.6 kcal/mol) to 1.56 eV (36.0 kcal/mol). This difference can be explained by another van der Waals DFT functional (DRSLL [26]) computation used by Correa and Orellana [21] under almost identical parameters of the quantum-chemical calculations. BH functional computation used in this work is the later version of DRSLL where the exchange part has already been modified [28]. The values of CuPc and ZnPc binding energies with CNT(10,0) estimated here are also lower that those presented by Basiuk *et al*. [22]. The difference can be explained again by another method used by these authors, which was PBE functional [33] with Grimme's empirical correction [34] and Gaussian double zeta plus polarization function (DNP) basis set. Another important reason is that we used the BSSE correction that decreases considerably the values of binding energy.

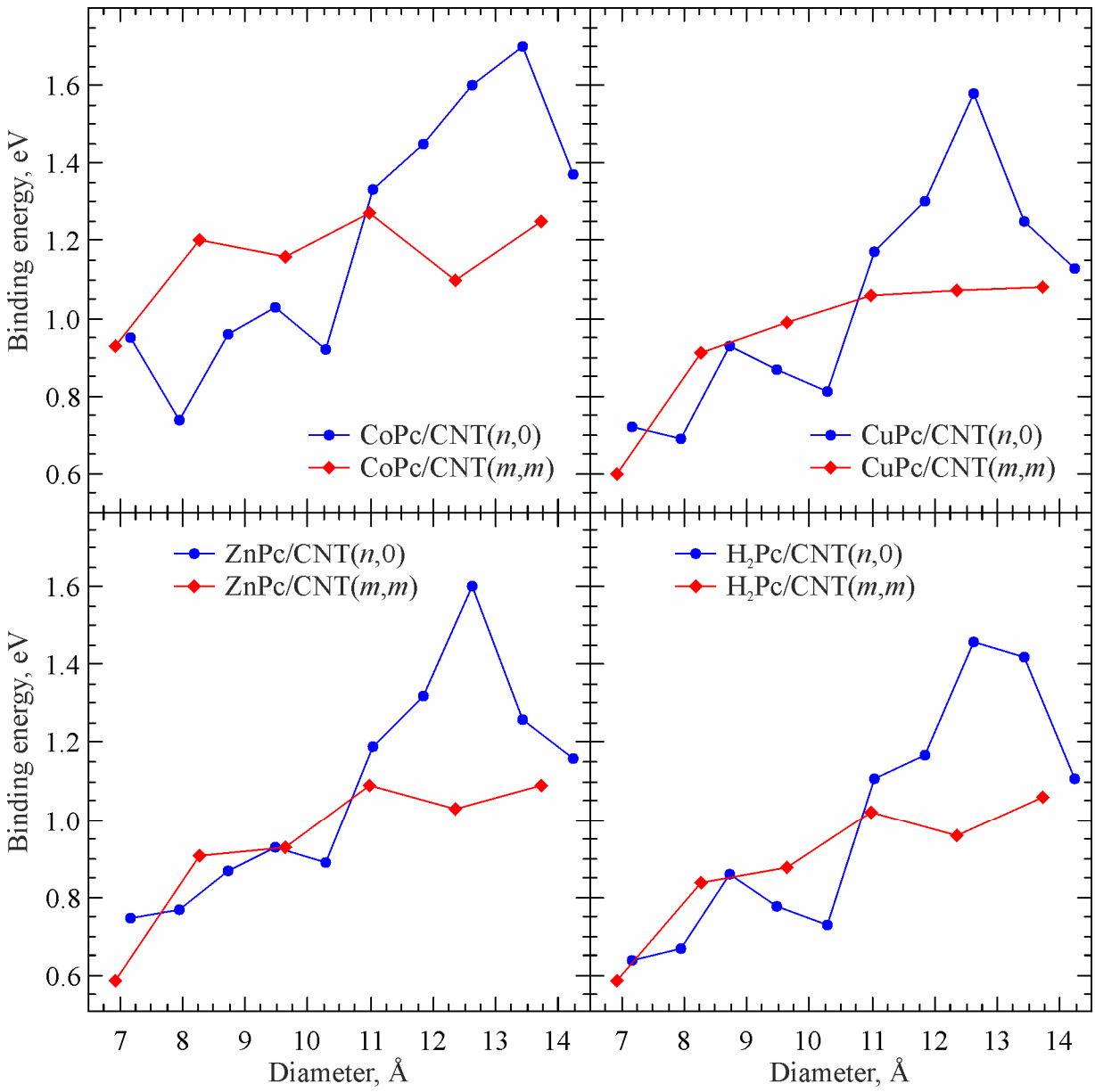

Figure 2 – Dependence of binding energy on CNT diameter corresponding to the most favorable orientation of MPcs on carbon nanotubes surface

Position 2 (Fig. 1) is the most favorable orientation of MPcs on the surface of *armchair* carbon nanotubes. This makes them different from the aggregates with the *zigzag* carbon nanotubes. The MPcs binding energy also grows with the increase of CNT diameters (Table 3), but this growth is not so pronounced as in the case of *zigzag* carbon nanotubes. The other distinctive feature is the fact that MPcs strongly attach to CNT(*m*,*m*) if their diameter is less than ~10.5 Å , whereas in the case of larger diameters they form stronger bonds with CNT(*n*,0) (Fig. 2).

As in the case of *zigzag* CNT, the strength of CoPc binding with *armchair* carbon nanotubes is higher than that of H_2Pc. In contrast to the case of *zigzag* CNT, the binding energy is little bit higher for CuPc/CNT aggregates than that for ZnPc/CNTs.

Table 3 – Binding energies of MPcs with carbon *armchair* nanotubes in eV (in kcal/mol)

CNT	CoPc		CuPc		ZnPc		H_2Pc		
	Position 1	Position 2	Position 1	Position 2	Position 1	Position 2	Position 1	Position 2	Position 3
(5,5)	0.93 (21.4)	0.93 (21.4)	0.60 (13.8)	0.57 (13.1)	0.42 (9.69)	0.58 (13.4)	0.58 (13.4)	0.54 (12.5)	0.47 (10.8)
(6,6)	1.02 (23.5)	1.20 (27.7)	0.70 (16.1)	0.91 (21.0)	0.62 (14.3)	0.90 (20.8)	0.67 (15.5)	0.83 (19.1)	0.79 (18.2)
(7,7)	1.05 (24.2)	1.16 (26.8)	0.72 (16.6)	0.99 (22.8)	0.62 (14.3)	0.92 (21.2)	0.72 (16.6)	0.87 (20.1)	0.82 (18.9)
(8,8)	1.27 (29.3)	1.24 (28.6)	1.03 (23.8)	1.06 (24.4)	0.99 (22.8)	1.08 (24.9)	0.95 (21.9)	1.01 (23.3)	0.94 (21.7)
(9,9)	1.09 (25.1)	1.10 (25.4)	1.02 (23.5)	1.07 (24.7)	1.00 (23.1)	1.02 (23.5)	0.95 (21.9)	0.93 (21.4)	0.85 (19.6)
(10,10)	1.08 (24.9)	1.25 (28.8)	0.78 (18.0)	1.08 (24.9)	0.74 (17.1)	1.08 (24.9)	0.68 (15.7)	1.05 (24.2)	0.96 (22.1)

The energy of MPcs interaction with the carbon nanotubes is comparatively high (0.44-1.45 eV or 10.1-33.4 kcal/mol) and comparable with the energy of a chemical bond (Tables 2 and 3, Fig. 2). In fact it is worth mentioning that there are no covalent bonds between MPc and CNT in their aggregates. The only binding however, is due to π-orbitals overlapping, as demonstrated by the low displacement of the electron density from carbon nanotubes to H_2Pc. This can be estimated from the total effective charge q(CNT) of CNT atoms, calculated according to the Hirshfeld method [35] in the corresponding supercells (Fig. 3). It is important to note that the only case when the value of q(CNT) is negative happens to the MPc/CNT(9,0) aggregate with MPc molecule in the Position 1.

The high value of binding energy of H_2Pc with CNTs is determined by the large area of their interaction, resulting in the MPc structure distortion (Fig. 1), as has already been described elsewhere [19-21]. At the same time, taking into account that H_2Pc molecule consists of 58 atoms, the binding energy with CNT per each atoms in a rough approximation is equal to 0.008-0.025 eV (0.18-0.58 kcal/mol). Such values correspond to the energy of π-π-interaction.

The bending of phthalocyanine molecules was estimated as $1/R$, where R is the radius of the circle passing through the z-coordinates of MPc (Fig. 4). In this case the distances l between the terminal hydrogen atoms and h between their mass centers and pyrrole nitrogen atoms can be

calculated using the coordinates of these atoms. It was shown that MPc molecule bending decreases with the increase in the diameter of carbon nanotubes (Tables S2 and S3, Supplementary Material).

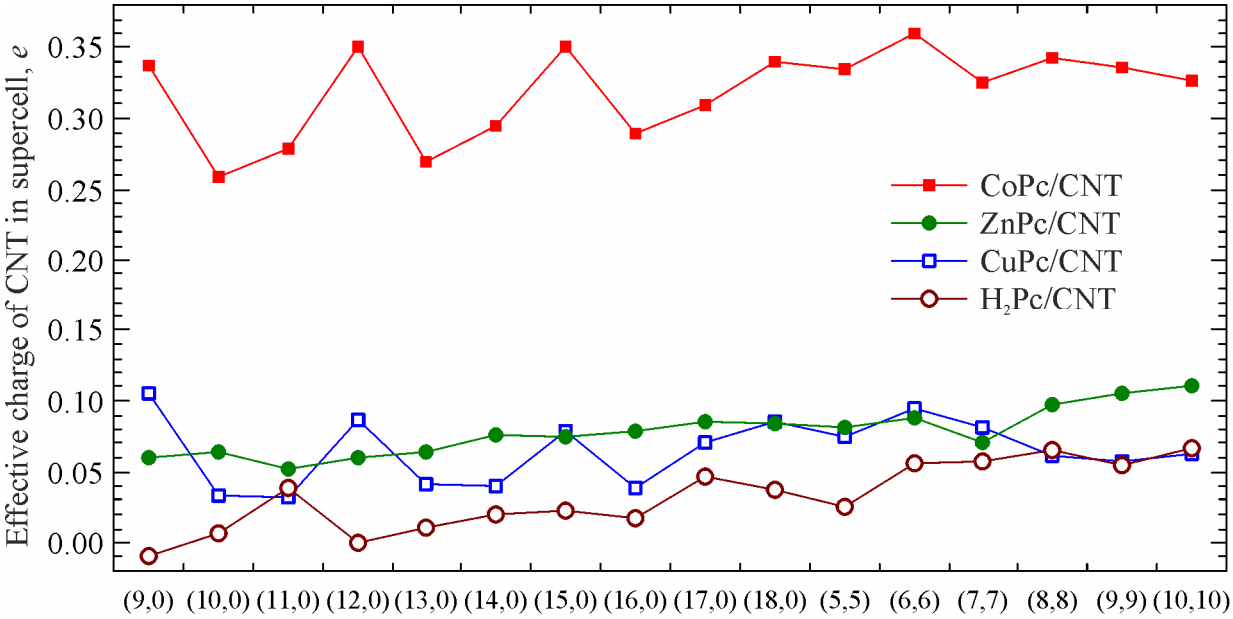

Figure 3 – Total effective charges of CNT atoms in supercells in the case of the most preferable orientations of MPcs on CNT surface

The distance ($d_{MPc/CNT}$) from carbon surface to MPc molecule, which is defined as the distance between CNT mass centers and pyrrole nitrogen atoms minus CNT radius (r_{CNT}), does not depend on the carbon nanotube diameter (Table S4 and S5, Supplementary Material). It rather depends mostly on MPc orientation, nature of the central metal and CNT chirality, and varies from 2.73 Å to 3.07 Å.

In the case of metals phthalocyanines, their binding energy with carbon nanotubes is higher compared to H_2Pc. However, in the calculation per one atom of MPc its value still remains comparable with the energy of π-π-interaction, whereas the electron density shift from CNT to MPc becomes more significant (Fig. 3). It is worth mentioning that in CoPc and CuPc aggregates with *armchair* CNTs and CNT(n,0) (where n is multiple of 3) the total effective charge of CNT carbon atoms in the supercell is larger than in the case of others *zigzag* CNTs. This behavior can be explained by the fact that the carbon nanotubes mentioned here are metallic or quasi-metallic, and they appear to exhibit better electron-donor activity. In the case of CuPc and H_2Pc aggregates with CNT(n,0) (where n = 9, 12, 15 and 18) such regularity is not observed, although *armchair* carbon nanotubes possess a slightly higher q(CNT) values in comparison with *zigzag* CNTs with close diameters.

It is worthwhile mentioning here that in most cases q(CNT) values increase in the order H_2Pc/CNT < CuPc/CNT < ZnPc/CNT < CoPc/CNT and they are considerably higher in CoPc aggregates (Fig. 3).

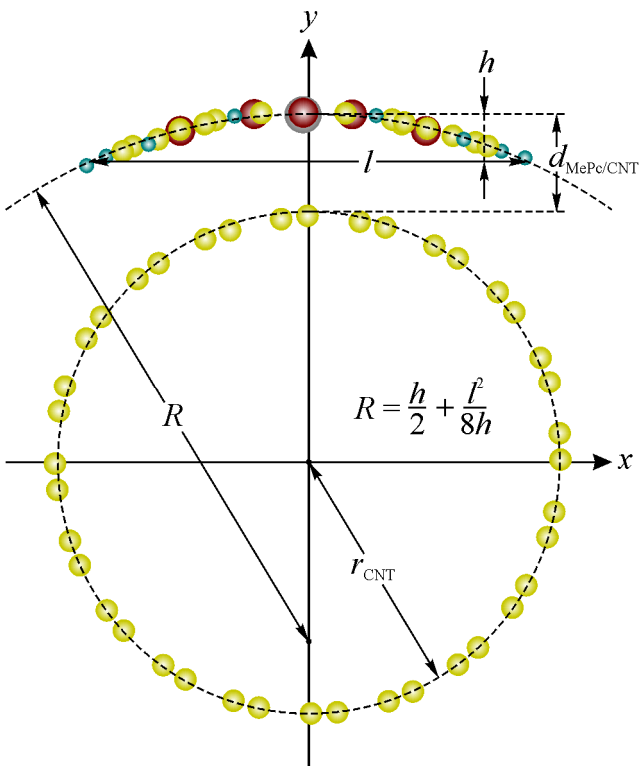

Figure 4 – Estimate of MPc bending on the CNT surface

On the one hand, the above-computed results appear to determine the stronger binding of CoPc with carbon nanotubes compared to phthalocyanines of other metals. This can be explained by the higher value of electron affinity of CoPc, calculated as the difference of total energies of the neutral molecule and anion. The electron affinity value of CoPc was calculated using the DFT BH/DZP method to be 2.82 eV, while very close values of 2.18 eV, 2.18 eV and 2.19 eV were computed for ZnPc, CuPc and H_2Pc, respectively.

4. Conclusion

Quantum-chemical calculations were performed of the geometrical structure and nature of the binding of carbon nanotubes with diameters ranging from 7 Å to 14 Å with phthalocyanine and its metal complexes. It was established that their interaction energy depends on many parameters, including CNT diameters, chirality of CNTs, phthalocyanines orientation on the surface and the nature of central the metal atom. The strength of MPc binding increases in the order H_2Pc/CNT < CuPc/CNT < ZnPc/CNT < CoPc/CNT. It was shown that the noncovalent binding of these aromatic molecules with the investigated carbon nanomaterials is due to π-π-interaction. This follows from the small values of binding energy per atom of a phthalocyanine molecule and the total effective charges of the carbon nanotube atoms in supercell.

A shift of electron density from carbon nanotubes to phthalocyanines was observed at the formation of MPc/CNT aggregates. The largest shift was observed in the case of CNT(m,m) as well as in the aggregates of CoPc and CuPc with CNT(n,0), where n is multiples of 3. It was shown that the interaction energy, as a whole, increases with an increase of the diameter of carbon nanotubes.

However, in the case of CNT(n,0) it reaches its maximal value at n = 16 or 17 depending on the central metal atom and phthalocyanine orientation on the carbon nanotube surface.

The position in which N-H or N-M bonds form the angle of 45º with the carbon nanotube axis is the most favorable orientation of MPcs in most aggregates with CNT(n,0). In the case of aggregates with CNT(m,m) the MPc molecules are located mainly so that the considered N-H and N-M bonds are parallel to the CNT axis. It is worth pointing out that in the case of aggregates with CNTs with small diameters (up to 10.5 Å) the stronger MPc binding is observed with *armchair* carbon nanotubes, whereas in the case of CNT with bigger diameters the phthalocyanines interact more strongly with *zigzag* CNTs.

5. Acknowledgements

The authors are grateful to the Data-Computing Center of Novosibirsk State University for the provision supercomputer facility. B.T.V. acknowledges FASO of Russian Federation for a financial support (project 0300-2016-0007).

6. References

[1] F. D'Souza, O. Ito, Supramolecular donor-acceptor hybrids of porphyrins/phthalocyanines with fullerenes/carbon nanotubes: electron transfer, sensing, switching, and catalytic applications, Chem. Commun. 33 (2009) 4913-4928.

[2] T. Hasobe, Supramolecular nanoarchitectures for light energy conversion, Phys. Chem. Chem. Phys. 12 (2010) 44-57.

[3] G. Bottari, J.A. Suanzes, O. Trukhina, T. Torres, Phthalocyanine-carbon nanostructure materials assembled through supramolecular interactions, J. Phys. Chem. Lett. 2 (2011) 905-913.

[4] G. Bottari, O. Trukhina, M. Ince, T. Torres, Towards artificial photosynthesis: Supramolecular, donor-acceptor, porphyrin and phthalocyanine/carbon nanostructure ensembles, Coord. Chem. Rev. 256 (2012) 2453-2477.

[5] T. Hasobe, Photo- and electro-functional self-assembled architectures of porphyrins, Phys. Chem. Chem. Phys. 14 (2012) 15975-15987.

[6] F. D'Souza, O. Ito, Photosensitized electron transfer processes of nanocarbons applicable to solar cells, Chem. Soc. Rev. 41 (2012) 86-96.

[7] O. Ito, F. D'Souza, Recent advances in photoinduced electron transfer processes of fullerene-based molecular assemblies and nanocomposites, Molecules 17 (2012) 5816-5835.

[8] B.I. Kharisov, O.V. Kharisova, Coordination and organometallic compounds in the functionalization of carbon nanotubes, J. Coord. Chem. 67 (2014) 3769-3808.

[9] B. Girek, W. Sliwa, Hybrids of cationic porphyrins with nanocarbons, J. Incl. Phenom. Macrocycl. Chem. 82 (2015) 283-300.

[10] C.B. KC, F. D'Souza, Design and photochemical study of supramolecular donor-acceptor systems assembled via metal-ligand axial coordination, Coord. Chem. Rev. 322 (2016) 104-141.

[11] G. de la Torre, G. Bottari, T. Torres, Phthalocyanines and subphthalocyanines: perfect partners for fullerenes and carbon nanotubes in molecular photovoltaics, Adv. Energy Mater. 7 (2017) 1601700.

[12] O. Ito, Photosensitizing electron transfer processes of fullerenes, carbon nanotubes, and carbon nanohorns, Chem. Rec. 17 (2017) 1-38.

[13] V.A. Basiuk, F.F. Contreras-Torres, M. Bassiouk, E.V. Basiuk, Interactions of porphyrins with low-dimensional carbon materials, J. Comput. Theor. Nanosci. 6 (2009) 1383-1411.

[14] J.H. Zagal, S. Griveau, K.I. Ozoemena, T. Nyokong, F. Bedioui, Carbon nanotubes, phthalocyanines and porphyrins: attractive hybrid materials for electrocatalysis and electroanalysis, J. Nanosci. Nanotechnol. 9 (2009) 2201-2214.

[15] G. de la Torre, G. Bottari, T. Torres, Phthalocyanines and subphthalocyanines: perfect partners for fullerenes and carbon nanotubes in molecular photovoltaics, Adv. Energy Mater. 7 (2017) 1601700.

[16] E.N. Kaya, S. Tuncel, T.V. Basova, H. Banimuslem, A. Hassan, A.G. Gürek, V. Ahsen, M. Durmuş, Effect of pyrene substitution on the formation and sensor properties of phthalocyanine-single walled carbon nanotube hybrids, Sens. Actuators, B 199 (2014) 277-283.

[17] E.N. Kaya, T. Basova, M. Polyakov, M. Durmuş, B. Kadem, A. Hassan, Hybrid materials of pyrene substituted phthalocyanines with single-walled carbon nanotubes: structure and sensing properties, RSC Adv. 5 (2015) 91855-91862.

[18] J. Zhao, Y. Ding, Functionalization of single-walled carbon nanotubes with metalloporphyrin complexes: a theoretical study, J. Phys. Chem. C 112 (2008) 11130-11134.

[19] L. Alvarez, F. Fall, A. Belhboub, R. Le Parc, Y. Almadori, R. Arenal, R. Aznar, P. Dieudonné-George, P. Hermet, A. Rahmani, B. Jousselme, S. Campidelli, J. Cambedouzou, T. Saito, J.-L. Bantignies, One-dimensional molecular crystal of phthalocyanine confined into single-walled carbon nanotubes, J. Phys. Chem. C 119 (2015) 5203-5210.

[20] E. Chávez-Colorado, V.A. Basiuk, Noncovalent interactions of free-base phthalocyanine with elongated fullerenes as carbon nanotube models, Struct. Chem. 28 (2017) 1765-1773.

[21] J.D. Correa, W. Orellana, Optical response of carbon nanotubes functionalized with (free-base, Zn) porphyrins, and phthalocyanines: a DFT study, Phys. Rev. B 86 (2012) 125417.

[22] V.A. Basiuk, L.J. Flores-Sánchez, V. Meza-Laguna, J.O. Flores-Flores, L. Bucio-Galindo, I. Puente-Lee, E.V. Basiuk, Noncovalent functionalization of pristine CVD single-walled carbon nanotubes with 3*d* metal(II) phthalocyanines by adsorption from the gas phase, Appl. Surf. Sci. 436 (2018) 1123-1133.

[23] L.A. De Souza, A.M. Da Silva Jr., G.M.A. Junqueira, A.C.M. Carvalho, H.F. Dos Santos, Theoretical study of structure and non-linear optical properties of Zn(II) porphyrin adsorbed on carbon nanotubes, J. Mol. Struct. THEOCHEM 959 (2010) 92-100.

[24] V.A. Karachevtsev, E.S. Zarudnev, S.G. Stepanian, A.Yu. Glamazda, M.V. Karachevtsev, L. Adamowicz, Raman spectroscopy and theoretical characterization of nanohybrids of porphyrins with carbon nanotubes, J. Phys. Chem. C 114 (2010) 16215-16222.

[25] J. Braun, M. Schlabach, B. Wehrle, M. Köcher, E. Vogel, H.-H. Limbach, NMR study of the tautomerism of porphyrin including the kinetic HH/HD/DD isotope effects in the liquid and the solid state, J. Am. Chem. Soc. 116 (1994) 6593-6604.

[26] M. Dion, H. Rydberg, E. Schröder, D.C. Langreth, B.I. Lundqvist, Van der Waals density functional for general geometries, Phys. Rev. Lett. 92 (2004) 246401.

[27] G. Román-Pérez, J. M. Soler, Efficient implementation of a van der Waals density functional: application to double-wall carbon nanotubes, Phys. Rev. Lett. 103 (2009) 096102.

[28] K. Berland, P. Hyldgaard, Exchange functional that tests the robustness of the plasmon description of the van der Waals density functional, Phys. Rev. B 89 (2014) 035412.

[29] C. Neto, E.P. Muniz, R. Centoducatte, F.E. Jorge, Gaussian basis sets for correlated wave functions. Hydrogen, helium, first- and second-row atoms, J. Mol. Struct. THEOCHEM 718 (2005) 219-224.

[30] G.G. Camiletti, S.F. Machado, F.E. Jorge, Gaussian basis set of double zeta quality for atoms K through Kr: application in DFT calculations of molecular properties, J. Comp. Chem. 29 (2008) 2434-2444.

[31] J.M. Soler, E. Artacho, J.D. Gale, A. Garcia, J. Junquera, P. Ordejón, J. D. Sánches-Portal, The SIESTA method for *ab initio* order-*N* materials simulation, J. Phys.: Condens. Matter. 14 (2002) 2745-2779.

[32] H.J. Monkhorst, J.D. Pack, Special points for Brillouin-zone integrations, Phys. Rev. B 13 (1976) 5188-5192.

[33] J.P. Perdew, K. Burke, M. Ernzerhof, Generalized gradient approximation made simple, Phys. Rev. Lett. 77 (1996) 3865-3568.

[34] S. Grimme, Semiempirical GGA-type density functional constructed with a long-range dispersion correction, J. Comput. Chem. 27 (2006) 1787-1799.

[35] F.L. Hirshfeld, Bonded-atom fragments for describing molecular charge densities, Theor. Chim. Acta 44 (1977) 129-138.